Enhancing effect of 5-azacytidine on saline–alkaline resistance of *Akebia trifoliata* and underlying physiological and transcriptomic mechanisms (#106841)

First submission

Guidance from your Editor

Please submit by **30 Nov 2024** for the benefit of the authors (and your token reward) .

Structure and Criteria
Please read the 'Structure and Criteria' page for guidance.

Custom checks
Make sure you include the custom checks shown below, in your review.

Author notes
Have you read the author notes on the guidance page?

Raw data check
Review the raw data.

Image check
Check that figures and images have not been inappropriately manipulated.

If this article is published your review will be made public. You can choose whether to sign your review. If uploading a PDF please remove any identifiable information (if you want to remain anonymous).

Files

Download and review all files from the materials page.

8 Figure file(s)
1 Table file(s)

Custom checks

Systematic review or meta analysis

- Have you checked our policies?
- Is the topic of the study relevant and meaningful?
- Are the results robust and believable?

Structure and Criteria

Structure your review

The review form is divided into 5 sections. Please consider these when composing your review:

1. **BASIC REPORTING**
2. **EXPERIMENTAL DESIGN**
3. **VALIDITY OF THE FINDINGS**
4. General comments
5. Confidential notes to the editor

You can also annotate this PDF and upload it as part of your review

When ready submit online.

Editorial Criteria

Use these criteria points to structure your review. The full detailed editorial criteria is on your guidance page.

BASIC REPORTING

- Clear, unambiguous, professional English language used throughout.
- Intro & background to show context. Literature well referenced & relevant.
- Structure conforms to PeerJ standards, discipline norm, or improved for clarity.
- Figures are relevant, high quality, well labelled & described.
- Raw data supplied (see PeerJ policy).

EXPERIMENTAL DESIGN

- Original primary research within Scope of the journal.
- Research question well defined, relevant & meaningful. It is stated how the research fills an identified knowledge gap.
- Rigorous investigation performed to a high technical & ethical standard.
- Methods described with sufficient detail & information to replicate.

VALIDITY OF THE FINDINGS

- **Impact and novelty is not assessed.** Meaningful replication encouraged where rationale & benefit to literature is clearly stated.
- All underlying data have been provided; they are robust, statistically sound, & controlled.
- Conclusions are well stated, linked to original research question & limited to supporting results.

Standout reviewing tips

The best reviewers use these techniques

Tip	*Example*
Support criticisms with evidence from the text or from other sources	*Smith et al (J of Methodology, 2005, V3, pp 123) have shown that the analysis you use in Lines 241-250 is not the most appropriate for this situation. Please explain why you used this method.*
Give specific suggestions on how to improve the manuscript	*Your introduction needs more detail. I suggest that you improve the description at lines 57- 86 to provide more justification for your study (specifically, you should expand upon the knowledge gap being filled).*
Comment on language and grammar issues	*The English language should be improved to ensure that an international audience can clearly understand your text. Some examples where the language could be improved include lines 23, 77, 121, 128 – the current phrasing makes comprehension difficult. I suggest you have a colleague who is proficient in English and familiar with the subject matter review your manuscript, or contact a professional editing service.*
Organize by importance of the issues, and number your points	*1. Your most important issue* *2. The next most important item* *3. …* *4. The least important points*
Please provide constructive criticism, and avoid personal opinions	*I thank you for providing the raw data, however your supplemental files need more descriptive metadata identifiers to be useful to future readers. Although your results are compelling, the data analysis should be improved in the following ways: AA, BB, CC*
Comment on strengths (as well as weaknesses) of the manuscript	*I commend the authors for their extensive data set, compiled over many years of detailed fieldwork. In addition, the manuscript is clearly written in professional, unambiguous language. If there is a weakness, it is in the statistical analysis (as I have noted above) which should be improved upon before Acceptance.*

Enhancing effect of 5-azacytidine on saline–alkaline resistance of *Akebia trifoliata* and underlying physiological and transcriptomic mechanisms

Xiao Xu Bi [Equal first author, 1], **Kai Wang** [Equal first author, 1], **Xiao qin Li** [1], **Jiao Chen** [1], **Jin Yang** [1], **Jin Yan** [1], **Gui jiao Wang** [1], **Yong fu Zhang** [Corresp. 1]

[1] School of Agriculture and Life Sciences, Kunming University, Kunming, Yunnan, China

Corresponding Author: Yong fu Zhang
Email address: 123017360@qq.com

Saline-alkaline stress is a common problem in *Akebia trifoliata* cultivation. In this study, the enhancing effects of 5-azacytidine (5-AzaC) on the resistance of *A. trifoliata* to saline–alkaline stress and the underlying mechanisms were investigated. Plant height, stem diameter, biomass, root length, fresh weight of root, and root/shoot ratio of 6-month-old *A. trifoliata* seedlings were measured after saline–alkaline stress with or without 5-AzaC treatment. Moreover, the contents of photosynthetic pigments, malondialdehyde (MDA), H_2O_2, sodium, soluble sugar, and proline; activities of superoxide dismutase, peroxidase (POD), and catalase (CAT); and anatomical structures of root, stem, and leaf were assessed. Furthermore, comparative transcriptome sequencing was performed. The results demonstrated that growth and development of *A. trifoliata* were severely inhibited under saline–alkaline stress, suggesting that the seedlings were exposed to severe oxidative and osmotic stresses. Treatment with exogenous 5-AzaC could significantly relieve the symptoms of saline–alkaline stress in *A. trifoliata*. Under saline–alkaline stress, 5-AzaC could increase the stem diameter, biomass, root length, fresh weight of root, and root/shoot ratio and minimize damages to the anatomical structure. Moreover, absorption of Na^+ was reduced; ionic balance was maintained; POD and CAT activities were significantly improved; proline and soluble sugar contents increased, and H_2O_2 and MDA contents decreased. Transcriptome analysis revealed that 5-AzaC functioned via regulating KEGG pathways such as Plant hormone signal transduction, Phenylpropanoid biosynthesis, Photosynthesis, Amino sugar and nucleotide sugar metabolism, and Glutathione metabolism under saline–alkaline stress. Particularly, enhanced expression of genes from the auxin pathway in Plant hormone signal transduction; the lignin synthetic pathway in Phenylpropanoid biosynthesis; and photosystem II, photosystem I, photosynthetic electron transport, and F-type ATP pathway in Photosynthesis may be related to 5-AzaC-induced

saline–alkaline resistance. The results provided theoretical references for *A. trifoliata* cultivation in saline–alkaline soil and application of 5-AzaC to improve saline–alkaline tolerance in plants.

Enhancing effect of 5-azacytidine on saline–alkaline resistance of *Akebia trifoliata* and underlying physiological and transcriptomic mechanisms

Xiaoxu Bi[1], Kai Wang[1], Xiaoqin Li[1], Jiao Chen[1], Jin Yang[1], Jin Yan[1], Guijiao Wang[1], Yongfu Zhang[1,*]

[1]College of Agronomy and Life Sciences, Kunming University, Kunming, 650214, China; Corresponding author(123017360@qq.com)orcid.org/0000-0001-5183-0731

Abstract

Saline-alkaline stress is a common problem in *Akebia trifoliata* cultivation. In this study, the enhancing effects of 5-azacytidine (5-AzaC) on the resistance of *A. trifoliata* to saline–alkaline stress and the underlying mechanisms were investigated. Plant height, stem diameter, biomass, root length, fresh weight of root, and root/shoot ratio of 6-month-old *A. trifoliata* seedlings were measured after saline–alkaline stress with or without 5-AzaC treatment. Moreover, the contents of photosynthetic pigments, malondialdehyde (MDA), H_2O_2, sodium, soluble sugar, and proline; activities of superoxide dismutase, peroxidase (POD), and catalase (CAT); and anatomical structures of root, stem, and leaf were assessed. Furthermore, comparative transcriptome sequencing was performed. The results demonstrated that growth and development of *A. trifoliata* were severely inhibited under saline–alkaline stress, suggesting that the seedlings were exposed to severe oxidative and osmotic stresses. Treatment with exogenous 5-AzaC could significantly relieve the symptoms of saline–alkaline stress in *A. trifoliata*. Under saline–alkaline stress, 5-AzaC could increase the stem diameter, biomass, root length, fresh weight of root, and root/shoot ratio and minimize damages to the anatomical structure. Moreover, absorption of Na^+ was reduced; ionic balance was maintained; POD and CAT activities were significantly improved; proline and soluble sugar contents increased, and H_2O_2 and MDA contents decreased. Transcriptome analysis revealed that 5-AzaC functioned via regulating KEGG pathways such as Plant hormone signal transduction, Phenylpropanoid biosynthesis, Photosynthesis, Amino sugar and nucleotide sugar metabolism, and Glutathione metabolism under saline–alkaline stress. Particularly, enhanced expression of genes from the auxin pathway in Plant hormone signal transduction; the lignin synthetic pathway in Phenylpropanoid biosynthesis; and photosystem II, photosystem I, photosynthetic electron transport, and F-type ATP pathway in Photosynthesis may be related to 5-AzaC-induced saline–alkaline resistance. The results provided theoretical

references for *A. trifoliata* cultivation in saline–alkaline soil and application of 5-AzaC to improve saline–alkaline tolerance in plants.

Key words: *Akebia trifoliata*, 5-azacytidine, saline-alkali stress, anatomical structure, Physiological and biochemical index, transcriptome analysis.

1. Introduction

Soil salinization has become a global problem affecting agricultural production in India, Australia, China, the United States, and more than 100 countries and regions. Salinized soil accounts for approximately 1/4th of the global land area, and due to natural and anthropogenic factors, saline–alkaline land area is increasing year by year (Gamalero et al. 2020, Zhang et al. 2022). Soil salinization is a very serious issue in the coastal and northwest regions of China, directly affecting agricultural production and development of China (Wu et al. 2019). Under the high-salt environment, plants are forced to absorb a large number of salt ions. Excessive salt ions disrupt the dynamic balance of the reactive oxygen metabolic system; this damages membrane lipids or membrane proteins, increases membrane permeability and intracellular water solute extravasation, and promotes physiological drought (Sadder et al. 2020). The damage caused to plants by saline–alkaline stress includes osmotic effects due to salt stress, ion imbalance, water deficiency, and nutrient deficiency, ultimately leading to oxidative stress in plants. Additionally, saline–alkaline stress may cause high-pH stress due to the presence of alkaline salts (Basu et al. 2020). Under saline–alkaline stress, plant cells exhibit increased production of reactive oxygen species (ROS) in the form of free radicals or non-free radicals. Excessive ROS production leads to oxidative damage of cellular proteins, lipids, nucleic acids, and plasma membrane; significant decrease in the uptake of phosphorus and potassium; and increase in the uptake of toxic ions such as Na^+ and Cl^-, negatively affecting the growth and yield of crops (Paheli et al. 2021, Keyikoglu et al. 2021).

Salt stress is very harmful to plant growth, and plants cannot escape from salt stress damage because their root system is fixed to the land. However, they have developed complex salt-resistance mechanisms in the long-term salt-stress environment. The common saline–alkaline resistance mechanisms include resistances to osmotic stress, oxidative stress, and ionic stress. First, under osmotic stress, plant roots accumulate small molecules, including proline, Na^+, K^+, NO_3^-, and soluble sugar, to regulate osmotic pressure in the plant and maintain the osmotic balance of cells and tissues (Latoyaharris et al. 2003). Further, under oxidative stress, activities of antioxidant enzymes such as superoxide dismutase (SOD), peroxidase (POD), and catalase (CAT) are enhanced, contributing to the removal of ROS (Wanget al. 2024). Additionally, when plants are subjected to saline–alkaline stress, intracellular Na^+

concentration decreases and K^+ concentration rapidly increases. As the extent of saline–alkaline stress increases, the Na^+/K^+ ratio in seedlings decreases. The presence of excessive Na^+ in plants leads to K^+ deficiency, inhibiting the uptake of other ions (Ca^{2+} and Mg^{2+}). Effective control of Na^+-K^+ uptake and transport can improve saline–alkaline resistance (Hamada et al. 2016, Zhu et al. 2016, Zhu et al. 2016).

It has been demonstrated that 5-azacytidine (5-AzaC), as a methylation inhibitor, enables plants to acquire new traits and generate new functions. 5-AzaC treatment in *Brassica oleracea var. botrytis* L. (Li et al. 2010) and *Rhododendron simsii* Planch. (Zhou et al. 2016) could reduce the DNA methylation level and promote early flowering. 5-AzaC treatment could slow down the growth of *B. rapa var. glabra* Regel seedlings under high-temperature stress, slow down the reduction in protein content and POD activity, and reduce the malondialdehyde (MDA) content and cell membrane permeability (Zhong et al. 2013). Additionally, 5-AzaC treatment improved salt resistance in wheat (Zhong et al. 2010), *Arabidopsis thaliana (L.)* Heynh. (Ogneva et al. 2019), and *Hibiscus cannabinus* L. (Li et al. 2021) under salt stress. However, it is unclear whether 5-AzaC improves salt resistance in *Akebia trifoliata*.

A. trifoliata (Thunb.) Koidz., with important value as a medicine and food, exhibits advantages including high yield, drought resistance, extensive growth management, and easy transplantation and planting. Its fruits are unique in taste and rich in sugar, vitamin C, and 12 amino acids. They can be used as raw materials for brewing and preparations of health food, fruit tea, and preserved fruits. Therefore, *A. trifoliata* has high nutritional and economic value. *A. trifoliata* is susceptible to saline–alkaline stress, which decrease the contents of soluble sugar, chlorophyll, and carotenoid. This negatively affects the growth and development of *A. trifoliata* and taste of its fruit.

In this study, the effect of 5-AzaC on the resistance of *A. trifoliata* to saline–alkaline stress was investigated. The roots of *A. trifoliata* were subjected to saline–alkaline stress with or without 5-AzaC treatment, and the morphology, physiological and biochemical responses, anatomical structure, non-parametric transcriptome sequencing, and bioinformatic analysis of the sequencing results were performed to reveal the effect and mechanism of action of 5-AzaC. This study provided technical support for the optimal growth and development of *A. trifoliata* in saline–alkaline soil and references for the analysis of related functional genes and molecular breeding in future.

2. Materials and methods

2.1 Materials and sample preparation

For this study, 6-month-old cuttings of *A. trifoliata* seedlings were obtained from Qiubei County, Wenshan

Prefecture, Yunnan Province. The experiment was conducted in the Agricultural Practice Park of Kunming College, Kunming, Yunnan Province. The process of cultivation was as follows. The lignified branches from winter pruning were cut. The morphological upper and lower ends were cut with flat and slant cuts, respectively. Overall, 2–3 axillary buds were retained in each branch. The morphological lower end was inserted into a seedling bag containing substrate (peat:vermiculite:perlite = 3:1:1). When the seedlings grew to 40–50 cm, healthy and uniformly grown seedlings free from pests and diseases were selected and planted in a bowl (diameter = 25 cm, height = 30 cm) with substrate (one plant per bowl). They were watered with 500 mL of Hoagland's solution (pH = 6.5) once a week. After 15 days, pests- and disease-free plants with uniform growth were selected and placed in white pots (100 cm × 35 cm × 35 cm) along with the contents of bowl. Four plants were placed in each pot. These pots were used for further treatments.

Three treatments were set up: Con (blank control), Salt (150 mmol/L Na^+), and Salt+5-AzaC (200 μmol/L 5-AzaC + 150 mmol/L Na^+). Each treatment involved three biological replicates. 5-AzaC (klamar; purity = 98%) was dissolved in sterile water to prepare 100 mmol/L solution, which was diluted 1000-folds for use. Sodium salts (Na_2SO_4:Na_2CO_3:$NaHCO_3$ = 1:1:1) were dissolved in Hoagland's solution to prepare a solution with Na^+ concentration of 150 mmol/L (pH = 8.5). For the Salt and Salt+5-AzaC groups, 1 L of this salt solution was poured in the white pots once a week. For the Salt+5-AzaC group, at the same time, each plant was uniformly sprayed with 100 μmol/L 5-AzaC on the front and back of the leaves and stem after every 3 days. For the Con group, the plants were treated with clean water. The morphology and physiological indexes were determined after 30 days of treatment.

2.2 Assessment of changes in morphology

The plant height, stem diameter, root length, biomass, fresh weight of root, and root/shoot ratio of *A. trifoliata* were measured. The aboveground height of plants was measured using a tape measure. The stem diameter was measured using a vernier calipers at a distance of 2 cm from the ground. Plants were pulled out from the substrate, washed with clean water, and dried at room temperature. Fresh weights of the above- and belowground parts were measured. The root/shoot ratio was calculated as: belowground fresh weight/aboveground fresh weight ×100%.

2.3 Measurement of physiological indexes and sodium content

Na^+ content was measured using bromocresol green spectrophotometry (Xi et al. 1998). Chlorophyll and carotenoid contents were measured using a method reported earlier (Dai et al. 2009). The contents of soluble sugar, SOD, H_2O_2, and free proline and POD and CAT activities were measured using sulfuric acid–phenol method, nitro-

blue tetrazolium photo-oxidation method, titanium sulfate colorimetric method, acidic ninhydrin chromogenic method, guaiacol–H_2O_2 chromogenic method, and UV absorption method, respectively (Lin et al. 2012). MDA content was determined using the thiobarbituric acid method (Zoltan et al. 2011).

2.4 Assessment of changes in the anatomical structure of root, stem, and leaves of *A. trifoliata*

The root, stem, and leaves of plants from the three groups were cut after 30 days of treatment. Root samples were collected from 5 cm below the rhizome; small leaves in the middle of the ternately compound leaf at the leaf position were collected as the leaf samples, and stem samples was collected from the middle of the stem. All samples were quickly immersed in FAA solution for fixation. Further, the samples were dehydrated with 75%, 85%, 95%, and 100% ethanol for 2 h each and further subjected to treatment with 1/2 anhydrous ethanol + 1/2 xylene (1.5 h), 1/3 anhydrous ethanol + 2/3 xylene (1.5 h), xylene (5 h), and xylene (1 h) to turn the samples transparent. Further, the samples were dipped in wax, sliced, dewaxed, stained with toluidine blue, decolored, stained with Fast Green FCF, decolorized, and finally examined microscopically using a orthostatic optical microscope (NIKON ECLIPSE E100, Japan). The images were acquired and data were analyzed using an imaging system (NIKON DS-U3).

2.5 Transcriptome sequencing

Total RNA was extracted from *A. trifoliata* leaves using a total RNA extraction kit (MJZol, Shanghai Major Biomedical Technology Co., Ltd.). The purity and integrity of RNA were determined using a Nanodrop 2000 spectrophotometer (Thermo Fisher Scientific, USA) and agarose gel electrophoresis, respectively. RIN was determined using a biological analyzer (Agilent 5300, USA). After passing the test, the library construction and non-parametric transcriptome sequencing were commissioned to Shanghai Major Biomedical Technology Co., Ltd.

The raw reads obtained from sequencing were subjected to quality control. The reads with adapters, N ratio > 10% (indicating that base information could not be determined), all A bases, and low-quality reads (bases with a quality value of Qphred ≤ 20 accounting for >50% of the entire reads) were removed so that high-quality clean reads could be obtained for subsequent analysis. Next, Trinity software (https://github.com/trinityrnaseq/trinityrnaseq/wiki) was used to assemble the clean reads to obtain the transcripts. The longest transcript of each gene was taken as the unigene based on the transcript sequence, which was used as the reference sequence for subsequent analyses. The clean reads of each sample were further mapped back to the assembled transcriptome without error using bowtie2 software. 2012). The results of the bowtie2 mapping were further analyzed using RSEM software

(http://deweylab.github.io/RSEM/) to quantify the expression level of the genes with the quantitative index FPKM. Subsequently, differential expression analysis was performed using DESeq2 software (http://bioconductor.org/packages/stats/bioc/DESeq2/), and differentially expressed unigenes (DEGs) were screened using the criteria: FDR < 0.05 and $|\log_2 FC| \geq 1$. The differences among different groups were compared, and the KEGG pathway enrichment analysis was performed using the DEGs to obtain the biological functions and metabolic pathways that were significantly associated with the DEGs. The metabolic pathway with a corrected P value (P_{adjust}) < 0.05 was considered as a significant pathway.

2.6 Data processing

The results were expressed as mean value (from three experimental replicates) ± SD. The data were processed and analyzed using SPSS 19.0. Duncan's new multiple range test was performed. $p < 0.05$ indicated statistically significant differences. Graphs were plotted using GraphPad Prism 9 and Adobe Illustrator CS6.

3. Results and analysis

3.1 Effects of 5-AzaC on the morphology of *A. trifoliata* under saline–alkaline stress

To investigate the effects of 5-AzaC on the morphology of *A. trifoliata* under saline–alkaline stress, various morphological indicators were examined. In the Salt group, the leaves were sparse and yellow, indicating a withered state; the main root of the root system was clearly shortened and blackened, and the fibrous root was significantly decayed and decreased compared with the Con group (Fig. 1). The leaf morphology of the Salt+5-AzaC group was normal; the leaves were green; the fibrous roots were fewer and shorter than those of the Con group but more in number and longer than those of the Salt+5-AzaC group. This demonstrated that 5-AzaC treatment could alleviate the dysplasia of the root system caused by saline–alkaline stress. Additionally, the stem diameter, biomass, root length, fresh weight of root, and root/shoot ratio exhibited the trend Con group > Salt+5-AzaC group > Salt group. This demonstrated that saline–alkaline stress treatment affected the stem diameter, biomass, root length, fresh weight of root, and root/shoot ratio. This might be attributed to the fact that saline–alkaline stress leads to reduced lengths of main roots and fibrous roots, which directly affect nutrient uptake and transport, thus affecting the growth and development of the whole plant. However, 5-AzaC could significantly alleviate the symptoms of saline–alkaline stress in *A. trifoliata*.

3.2 Effects of 5-AzaC on the physiological indexes of *A. trifoliata* under saline–alkaline stress

Compared with the Con group, Na^+ content in the leaves significantly increased and decreased in the Salt and Salt+5-AzaC groups, respectively (Fig. 2), demonstrating that 5-AzaC could reduce the uptake and enrichment of Na^+ by plants. The activities of CAT, POD, and SOD were significantly lower in the Salt group than in the Con group. Compared with the Salt group, CAT and POD activities significantly increased in the Salt+5-AzaC group; however, the SOD activity was comparable. Therefore, saline–alkaline stress treatment severely inhibited the activities of CAT, POD, and SOD in the leaves of *A. trifoliata*, whereas 5-AzaC treatment significantly increased CAT and POD activities under saline–alkaline stress. MDA and H_2O_2 contents were significantly lower in the Con group than in the Salt group. MDA and H_2O_2 contents significantly increased after treatment with 5-AzaC under saline–alkaline stress. Compared with the Con group, soluble sugar content slightly increased and proline content significantly increased in the Salt group, whereas both contents significantly increased in the Salt+5-AzaC group. The contents of chlorophyll a, chlorophyll b, total chlorophyll, and carotenoid significantly reduced in the Salt group. Their contents were significantly higher in the Salt+5-AzaC group than in the Salt group. These results indicated that excessive Na^+ entered *A. trifoliata* under saline–alkaline stress, affected its enzyme activity, and interfered with its normal physiological metabolism and life activities, leading to the accumulation of a large amount of toxic substances such as MDA and H_2O_2 in the cells. This caused osmotic stress and oxidative damage; reduced the contents of chlorophyll a, chlorophyll b, total chlorophyll, and carotenoid; and affected photosynthesis. However, Na^+ restored the equilibrium state after 5-AzaC treatment; this increased the contents of soluble sugar, proline, and photosynthetic pigments and CAT and POD activities compared with saline–alkaline stress conditions, which reduced MDA and H_2O_2 contents to a certain extent. Therefore, 5-AzaC treatment could effectively reduce the damage to *A. trifoliata* due to saline–alkaline stress.

3.3 Effects of 5-AzaC on the anatomical structure of *A. trifoliata* under saline–alkaline stress

Root cross-section diameter, cortex thickness, phloem thickness, and xylem catheter aperture increased under saline–alkaline stress (Figs. 3A–C). The root cross-section diameter and xylem catheter aperture significantly increased by 65.92% and 56.80%, respectively, in the Salt+5-AzaC group ($P < 0.05$) compared with those in the Salt group. Compared with the Con group, the root cross-section diameter, cortex thickness, phloem thickness, and xylem catheter aperture increased in the Salt group, with the root cross-section diameter and phloem thickness exhibiting significant increase ($P < 0.05$) by 43.50% and 126.72%, respectively, with no significant effect on the xylem and cambium (Fig. 3J). Therefore, spraying of 200 μmol/L 5-AzaC under saline–alkaline stress could promote lateral root

191 growth and phloem thickening, increase the xylem catheter aperture to enhance the transport efficiency, and weaken
192 the damage due to saline–alkaline stress on the root system of *A. trifoliata*.

193 Compared with that of the Con group, the stem cambium thickness increased by 50.46% and cortex thickness,
194 phloem thickness, xylem catheter aperture, and medullary radius reduced by 130.68%, 30.73%, 28.05%, and 20.24%,
195 respectively, in the Salt+5-AzaC group. The differences in cortex thickness, phloem thickness, and medullary radius
196 were significant ($P < 0.05$). Compared with the Salt group, the Salt+5-AzaC group exhibited significantly improved
197 cortex thickness, phloem thickness, xylem catheter aperture, and medullary radius (by 49.47%, 49.72%, 55.42%, and
198 22.12%, respectively) ($P < 0.05$) (Figs. 3D, E, F, and K). Therefore, saline–alkaline stress injured the cortex of *A.*
199 *trifoliata* and resulted in the thinning of phloem and reduction of xylem catheter aperture and medullary radius, which
200 weakened the transport capacity of the stem and affected the normal physiological and metabolic activities. However,
201 spraying of 200 μmol/L 5-AzaC could effectively alleviate this phenomenon and enhance the transport capacity of *A.*
202 *trifoliata*.

203 The leaves of *A. trifoliata* are typical bifacial leaves, consisting of upper epidermal cells, lower epidermal cells,
204 palisade cells, and spongy tissue. The thickness of *A. trifoliata* leaves and upper and lower epidermis were reduced
205 under saline–alkaline stress (Fig. 3); Compared with the Con group, the Salt group exhibited decrease by 7.93%,
206 27.61%, 35.23%, 60.66%, and 97.93%, respectively, whereas the thickness of leaves and upper and lower epidermis
207 exhibited increase by 7.77% and 29.41% compared with the Con group after spraying of 200 μmol/L 5-AzaC.
208 Compared with the Salt group, the Salt+5-AzaC group exhibited significant increase (by 16.31%, 55.56%, 75%,
209 48.36%, and 78.86%, respectively) in the thickness of leaves, upper epidermis, lower epidermis, palisade cells, and
210 spongy tissue. Additionally, the ratio of palisade cells to spongy tissue was 0.96 in the Salt group, exhibiting increase
211 by 23.08% and 20% compared with the Con and Salt+5-AzaC groups, respectively. This demonstrated that the spongy
212 tissue in leaves of *A. trifoliata* increased in size, and the length of the palisade cells gradually decreased; the tissue
213 layer thinned; the arrangement became looser, and the intercellular space became larger and larger. The cells of the
214 spongy tissue gradually enlarged and changed from compact to lax; advanced air cavities appeared, and interstitial
215 spaces were gradually developed. Overall, spraying of 200 μmol/L 5-AzaC under saline–alkaline stress could alleviate
216 various damages caused by saline–alkaline stress by increasing the thickness of *A. trifoliata* leaves and upper and
217 lower epidermis.

3.4 Effects of 5-AzaC on the transcriptome of *A. trifoliata* under saline–alkaline stress

The effect of 5-AzaC on *A. trifoliata* at the gene level was investigated under saline–alkaline stress. Using transcriptome sequencing, 51.84 Gb clean bases and 3.52 G clean reads were obtained from 9 samples from 3 groups of samples with 3 replicates. The average output of each sample was 6.48 Gb clean bases and 0.44 G clean reads. The GC content of each sample was 42.97%–44.06%, and the percentage of Q20% and Q30% bases exceeded 94% (Table 1). The accuracy of the measured data was high, which met the requirements of quality control and facilitated data analysis in the later stage. Based on the quantitative results, inter-group DEG analysis was performed to obtain the DEGs between the two groups. The threshold range of $|\log_2 FC| \geq 1.00$ and P-adjust ≤ 0.05 were selected for the analysis of the difference using DESeq2 to identify the DEGs of different groups. The visualization analysis results using a bar chart (Fig. 4B) indicated 8253, 4459, and 3035 DEGs in the Salt vs Con, Salt+5-AzaC vs Con, and Salt+5-AzaC vs Salt groups, respectively. Among them, 3667, 2283, and 1859 DEGs were upregulated and 4586, 2176, and 1176 DEGs were downregulated. A total of 3264, 815, and 1854 DEGs were observed between the Salt+5-AzaC vs Con and Salt vs Con, Salt+5-AzaC vs Con and Salt+5-AzaC vs Salt, and Salt vs Con and Salt+5-AzaC vs Salt groups, respectively. In total, 413 DEGs were observed in the three groups. Overall, 793, 3548, and 779 unique DEGs were observed in the Salt+5-AzaC vs Con, Salt vs Con, and Salt+5-AzaC vs Salt groups, respectively (Fig. 4A). The shared genes may have occurred due to the common environment, whereas the unique ones may be in response to different treatments.

3.5 KEGG pathway enrichment analysis of the DEGs involved in the effects of 5-AzaC on *A. trifoliata* under saline–alkaline stress

In Salt vs Con, 935 DEGs were enriched in the KEGG pathway (Fig. 5). Among them, Plant hormone signal transduction (map04075), Oxidative phosphorylation (map00190), Amino sugar and nucleotide sugar metabolism (map00520), Phenylpropanoid biosynthesis (map00940), Photosynthesis (map00195), Sesquiterpenoid and triterpenoid biosynthesis (map00909), Fatty acid biosynthesis (map00061), and Fatty acid elongation (map00062) had the highest number of enriched DEGs (n = 116, 84, 58, 54, 41, 23, 21, and 18, respectively). In Salt+5-AzaC vs Con, 1462 DEGs were enriched in the KEGG pathway. The pathways with the highest number of DEGs (60, 45, and 37) were Plant hormone signal transduction (map04075), Amino sugar and nucleotide sugar metabolism (map00520), and Phenylpropanoid biosynthesis (map00940), respectively. In Salt+5-AzaC vs Salt, 935 DEGs were enriched in the

KEGG pathway with the highest number of genes (28, 12, 23, and 6) enriching in Photosynthesis (map00195), Photosynthesis - antenna proteins (map00196), Glutathione metabolism (map00480), and Flavone and flavonol biosynthesis (map00944), respectively.

The DEGs between Salt+5-AzaC vs Salt and Salt+5-AzaC vs Con were mainly enriched in metabolic pathways. The number of DEGs was higher in Salt+5-AzaC vs Con than in Salt+5-AzaC vs Salt. This suggested that 5-AzaC could stimulate more metabolic response mechanisms under saline–alkaline stress in *A. trifoliata*, enhance the metabolic capacity of plants, and thus alleviate the damage caused by saline–alkaline stress to *A. trifoliata*, promoting the development of *A. trifoliata*.

3.6 Key DEGs in *A. trifoliata* after 5-AzaC treatment under saline–alkaline stress

3.6.1 DEGs involved in Plant hormone signal transduction

KEGG pathway enrichment analysis indicated that in Salt vs Con and Salt+5-AzaC vs Con, the DEGS were highly enriched in Plant hormone signal transduction (Figs. 5A and B). Notably, most DEGs in Plant hormone signal transduction belonged to auxin synthetic pathway. Compared with the Con group, 65 DEGs in the Salt group were involved in auxin synthesis. Among them, 2, 2, 12, 44, and 1 DEGs were downregulated, which were responsible for encoding AUX1, GH3, IAA, SUAR, and TIR1, respectively (Fig. 6). This suggested that saline–alkaline stress can significantly inhibit auxin synthesis in *A. trifoliata*. Compared with the Salt group, the Salt+5-AzaC group contained 10 DEGs, of which 9 were upregulated. The 6 DEGs that are responsible for encoding SAUR were downregulated in the Salt group compared with the Con group. These 6 DEGs were upregulated in Salt+5-AzaC vs Salt. This demonstrated that 5-AzaC may regulate the auxin pathway in *A. trifoliata* by regulating the expression of SAUR, thus promoting growth of *A. trifoliata*, and improving its saline–alkaline resistance, which was consistent with the morphological and leaf anatomical observations of *A. trifoliata* after 5-AzaC treatment.

3.6.2 DEGs involved in Phenylpropanoid biosynthesis

Phenylpropanoid biosynthesis was also significantly enriched in Salt vs Con and Salt+5-AzaC vs Con (Figs. 5A and B). Several unigenes were involved in phenylpropanoid biosynthesis, including 4CL, E3.2.1.21, CAD, COMT, CSE, E1.11.1.7, E2.1.1.104, HCT, E3.2.1.21, REF1, TOGT1, and UGT72E (Fig. 7). Compared with the Con group, the Salt group had 54 DEGs. Among them, 14, 12, 2, 1, 2, 1, 1, 1, 1, and 1 DEGs that are responsible for encoding E1.11.1.7, E3.2.1.21, HCT, E2.1.1.104, 4CL, REF1, CSE, COMT, CAD, and TOGT1, respectively, were

downregulated. Meanwhile, 4, 2, 5, 1, 1, 1, 1, and 1 DEGs that are responsible for encoding E3.2.1.21, TOGT1, E1.11.1.7, HCT, CSE, CAD, 4CL, and UGT72E, respectively, were upregulated (Fig. 7). This suggested that most unigenes involved in Phenylpropanoid biosynthesis were downregulated under saline–alkaline stress. Compared with the Con group, the Salt+5-AzaC group had 10 new DEGs. Among them, 8 and 1 DEgs that are responsible for encoding E1.11.1.7 and E3.2.1.21, respectively, were upregulated (Fig. 7). This suggested that 5-AzaC may promote POD activity under saline–alkaline stress by specifically promoting the expression of E1.11.1.7, thereby enhancing the antioxidant capacity of *A. trifoliata*. This was consistent with the significant increase in POD activity after 5-AzaC treatment as described in section 3.2. Additionally, compared with the Salt group, the Salt+5-AzaC group had 19 DEGs. Among them, 18 were upregulated, and 5, 5, 1, 1, and 1 DEGs that are responsible for encoding E3.2.1.21, E1.11.1.7, REF1, COMT, and TOGT1, respectively, were downregulated in Salt vs Con (Fig. 7). This indicated that the enhanced expression of these unigenes may be related to the potential mechanism of 5-AzaC in enhancing saline–alkaline resistance of *A. trifoliata*.

3.6.3 DEGs participating in Photosynthesis

Photosynthesis was the most significantly enriched KEGG pathway in Salt+5-AzaC vs Salt (Fig. 5C). Many unigenes involved in Photosynthesis were affected by 5-AzaC. Compared with the Con group, the Salt group had 41 DEGs, of which 31 were downregulated (Fig. 8). Of these 31 DEGs, 1, 3, 1, 2, 2, 1, and 1 DEGs encoding psbA, psbQ, psbS, psbW, psbY, psb27, and psb28 related to photosystem II; 1, 1, 2, 1, 1, and 1 DEGs encoding psaD, psaE, psaG, psaH, psaK, and psaL related to photosystem I; 1 and 5 DEGs encoding petE and petF related to photosynthetic electron transport; and 1, 1, and 1 DEGs encoding atpF, atpG, and atpH related to F-ATPase, respectively, were downregulated in the Salt group (Fig. 8). However, these DEGs were upregulated in Salt vs. Salt+5-AzaC (Fig. 8). Therefore, photosynthesis of *A. trifoliata* was significantly inhibited by saline–alkaline stress, and this inhibition was ameliorated by 5-AzaC treatment.

4. Discussion

Soil salinization has become a serious global problem limiting agricultural development and is one of the major abiotic stresses limiting plant growth and development. Effective utilization of response mechanisms against saline–alkaline stress can help plants to withstand adverse environments (Fu et al. 2023). Saline–alkaline stress can cause a series of physiological and metabolic changes in plants, resulting in ionic stress, osmotic stress, and oxidative stress

and secondary damage (Yang et al. 2018). In practice, substances such as proline, betaine, sugar, NO, silicon, jasmonic acid, organic acids, and melanin can be applied exogenously to alleviate the damage caused by saline–alkaline stress (Ashraf et al. 2007, Zhao et al. 2015, Zhou et al. 2015, Liang et al. 2015, Ding et al. 2015, Jiang et al. 2016). Currently, relevant studies in China and abroad have mainly focused on the NaCl stress tolerance of plants (Li et al. 2009), and no report is available on the saline–alkaline stress resistance in *A. trifoliata*. Therefore, in this study, *A. trifoliata* was subjected to mixed saline–alkaline treatment using Na_2SO_4, $NaHCO_3$, and Na_2CO_3 solution, and the mechanism of action of 5-AzaC to alleviate the saline–alkaline stress was explored.

Structure is the basis of function, and anatomical structure characteristics of plants are the result of their response to the surrounding growth environment (Zhao et al. 2017). In this study, the leaves of *A. trifoliata* were thicker; palisade cells were developed; veins were well developed, and catheter aperture was larger in the Con group. Therefore, plants in the Con group grew vigorously, which could be attributed to following facts. Thicker leaves are more conducive to reducing excessive water evaporation; the development of palisade cells is closely related to the photosynthetic capacity, and well-developed leaf veins and larger catheter aperture are more conducive to the transport of water (Li et al. 2005, Dong et al. 2001). Under saline–alkaline stress, the leaves of *A. trifoliata* were thinned; the tissue structure was clearly damaged, and the palisade cells were deformed and disorganized. Compared with the Salt group, the leaves remained intact in the Salt+5-AzaC group; the thickness of the upper and lower epidermis was significantly high; the palisade cells were thickened, which improved the photosynthetic and water-transporting capacity. The root system is an important organ for water and nutrient uptake. Additionally, it is the first part of the plant that gets exposed to soil stress. The size of the aperture of the root xylem catheter directly affects the transport of radial water flow and efficiency of water utilization in the root system (Joseph et al. 2014). In this study, the xylem catheter aperture of *A. trifoliata* root was significantly thickened, and the phloem was significantly thinned under saline–alkaline stress. However, 5-AzaC treatment increased the root xylem catheter aperture, which was conducive to the improvement of water transport and utilization efficiency of the root system. Moreover, the phloem was further thickened to form a barrier, which could alleviate the entry of harmful ions into the roots. Additionally, compared with the Con group, the medullary radius of the stem was significantly reduced under saline–alkaline stress, which would be unfavorable to nutrient storage. This was consistent with a study on *Salicornia europaea* (Akcin et al. 2017), in which spraying of 5-AzaC restored the medullary radius reduced by saline–alkaline stress to a level close to that of

the control; this was conducive to nutrient storage, thus alleviating the injurious effects of saline–alkaline stress.

Under saline–alkaline stress, the excessive accumulation of Na^+ can easily lead to the damage of the cell membrane system, thus inducing oxidative stress (Zhu et al.2003). In this study, 5-AzaC treatment effectively reduced the Na^+ uptake by *A. trifoliata* and reduced the cellular damage caused by high Na^+ concentration, which helped to improve its resistance to saline–alkaline stress. Saline–alkaline stress causes chlorophyll degradation and affects photosynthesis, and chlorophyll content reflects the stress resistance of plants (Zhu et al. 2024). Our results were consistent with this. Under saline–alkaline stress, H_2O_2 and MDA can easily disrupt the metabolic balance of intracellular ROS, and the large amount of accumulated ROS can cause severe peroxidative damage to the plasma membrane (Jiang et al. 2019). SOD, POD, and CAT are the key indicators for measuring plant stress resistance (Gill et al. 2010). In this study, compared with the Con group, H_2O_2 and MDA contents in the leaves significantly increased and SOD, activities of POD and CAT significantly decreased under saline–alkaline stress in the Salt group. This demonstrated that saline–alkaline stress caused serious oxidative damage to the cell membrane of *A. trifoliata*. The total chlorophyll content and POD and CAT activities were significantly higher in the Salt-5+AzaC group than in the Salt group. Therefore, it was evident that 5-AzaC could effectively alleviate the effects of saline–alkaline stress on the membrane lipid peroxidation of *A. trifoliata*. Additionally, plants can use osmoregulation as a self-defense mechanism under stress, e.g., increasing soluble sugar and proline contents to maintain cellular osmotic pressure (Xu et al. 2020, Zhang et al. 2012). In this study, proline content in *A. trifoliata* leaves significantly increased under saline–alkaline stress, whereas the increase in the proline content in leaves increased after 5-AzaC treatment. This demonstrated that 5-AzaC could increase the resistance to saline–alkaline stress by increasing proline content in *A. trifoliata* leaves.

5-AzaC induced changes in the expression of genes involved in KEGG pathways such as Amino sugar and nucleotide sugar metabolism, Starch and sucrose metabolism, Oxidative phosphorylation, Glutathione metabolism, Phenylpropanoid biosynthesis, Phagosome, Photosynthesis, and Plant hormone signal transduction in *A. trifoliata* leaves, thus improving its saline–alkaline resistance. Particularly, most DEGs enriched in Plant hormone signal transduction pathway belonged to auxin synthetic pathway. Hence, 5-AzaC may mediate the saline–alkaline resistance of *A. trifoliata* mainly via altering the expression of DEGs in auxin synthetic pathway. In auxin synthesis, AUX/IAA and SAUR are the two most important early auxin-responsive gene families (He et al. 2019). The expression pattern of AUX/IAA gene family is relatively complex. For example, some AUX/IAA-encoding genes are involved in the

differentiation of *Dimocarpus longan* flower bud (Jue et al. 2019), and they regulate drought resistance in *Arabidopsis thaliana* (Estelle et al. 2019). As the largest gene family among the early auxin-responsive genes in plants (Shin et al. 2019), SAUR plays a key role in the resistance of plants to biotic and abiotic stresses. For example, overexpression of SAUR-encoding genes can lead to increased survival rates of *Triticum aestivum* under drought and salt stresses (Guo et al. 2018). In this study, most DEGs related to the auxin pathway belonged to the AUX/IAA and SAUR families, demonstrating that the auxin pathway plays a key role in the resistance of plants to saline–alkaline stress. This is consistent with the results of changes in the morphology and leaf anatomical structure of *A. trifoliata* after 5-AzaC treatment.

The roles of phenylpropane biosynthetic pathway in the resistance of plants to abiotic stress have been explored (Zhou et al. 2016, Zou et al. 2019). In this study, compared with the Salt group, the Salt+5-AzaC group had 19 DEGs (with 18 upregulated DEGs). Five DEGs encoding E1.11.1.7 were downregulated in Salt vs Con but upregulated in Salt+5-AzaC vs Salt. Hence, 5-AzaC may regulate the saline–alkaline resistance of *A. trifoliata* under saline–alkaline stress by regulating the expression of E1.11.1.7. This is consistent with significantly increased POD activity in *A. trifoliata* leaves. Additionally, E1.11.1.7 expression can significantly affect lignin biosynthesis (Qiu et al. 2021), which is of great significance as lignin improves plant stress resistance and tolerance (Sharma et al. 2020). Moreover, lignin accumulation facilitates the activation of plant defense systems in response to selective pressures from the environment (Yadav et al. 2020). Therefore, 5-AzaC treatment may improve the acid resistance of *A. trifoliata* by promoting lignin accumulation.

The effects of saline–alkaline stress on photosynthesis of plants have been thoroughly investigated (Ren et al. 2023, Ling et al. 2022). In this study, various unigenes involved in the KEGG pathway of photosynthesis, including photosystem II (PSII), photosystem I (PSI), photosynthetic electron transport, and F-ATPase, were affected by 5-AzaC. Under saline–alkaline stress, Na^+-induced oxidative stress disrupts the reaction center of PSII in plants, resulting in degraded activity of PSII (Zhang et al. 2002). Meanwhile, ROS accumulated in the chloroplast mainly inhibits the repair process of PSII by inhibiting protein synthesis in the PSII and mainly targets PsbA-encoded D1 protein (Chen et al. 2020). In this study, PsbA-encoding DEGs were upregulated, and chlorophyll content significantly increased after 5-AzaC treatment compared with saline–alkaline stress treatment alone. This suggested that 5-AzaC significantly positively affected stability maintenance and accumulation of photosynthetic pigments in PSII of *A.*

trifoliata under saline–alkaline stress. The iron–sulfur cluster in PSI receptor is the first site attacked by ROS. Abundant ROS scavengers (e.g., SOD and APX) are distributed in the vicinity to prevent ROS from spreading to the substrate and causing toxicity (Zhang et al. 2013). In this study, SOD and POD activities significantly decreased in the Salt group, and in Salt vs Con, DEGs encoding psaD, psaE, psaG, psaH, psaK, and psaL were significantly downregulated. This indicated that saline–alkaline stress inhibited the activity of ROS scavengers. After 5-AzaC treatment, POD and CAT activities were significantly increased, and DEGs encoding psaD, psaE, psaG, psaH, psaK, and psaL were significantly upregulated. As electron carriers on the electron transport chain, plastocyanin (PC) and ferredoxin (Fd) play a key role in photosynthetic electron transport and energy conversion (Magistretti et al. 1987). In this study, PetE-encoding DEGs in the PC protein and PetF-encoding DEGs in the Fd protein were downregulated under saline–alkaline stress compared with the Con group. After 5-AzaC treatment, these DEGs were upregulated, indicating that 5-AzaC-induced expression of petF may play a key role in reducing toxicity related to saline–alkaline stress in plants. F-ATPase located in the thylakoid membrane of chloroplast can catalyze the conversion of ADP to ATP, thereby providing energy for carbon fixation by plants (Kuhlbrandt et al. 2019). In this study, DEGs such as atpF, atpG, and atpH in the ATP synthetic pathway were downregulated under saline–alkaline stress but upregulated after 5-AzaC treatment. This indicated that 5-AzaC may promote ATP synthesis and provide energy for carbon assimilation. Overall, 5-AzaC has a potential role in protecting *A. trifoliata* from saline–alkaline stress. However, further studies are needed to explore more relevant signal transduction pathways involved in the action of 5-AzaC in enhancing the saline–alkaline resistance of plants.

5. Conclusion

Saline–alkaline stress severely inhibited the growth and development of *A. trifoliata*; however, exogenous 5-AzaC application could effectively alleviate the negative impacts of saline–alkaline stress on *A. trifoliata* in terms of stem diameter, root length, fresh weight of root, root/shoot ratio, and biomass. Specifically, 5-AzaC could increase the activity of antioxidant enzymes and content of osmoregulatory substances in *A. trifoliata* under saline–alkaline stress. H_2O_2 and MDA contents were reduced after 5-AzaC treatment, thus reducing osmotic stress and oxidative damage of *A. trifoliata* under saline–alkaline stress. Additionally, 5-AzaC could promote chlorophyll synthesis in *A. trifoliata* and protect photosynthetic systems from damage under saline–alkaline stress. Moreover, it could effectively reduce Na^+ uptake and regulate ionic homeostasis. Meanwhile, the increased expression of genes from auxin pathway

in Plant hormone signal transduction; lignin synthetic pathway in Phenylpropanoid biosynthesis; and PSII, PSI, photosynthetic electron transport, and F-ATPase pathway in Photosynthesis may be closely related to 5-AzaC-induced saline–alkaline resistance of *A. trifoliata*. This study provided references for using 5-AzaC to enhance the saline–alkaline resistance of *A. trifoliata* in practical applications.

6. Acknowledgments

The authors are grateful to the editors and the reviewers for their valuable comments and help. This work was supported by the Kunming University.

7. Additional information and declarations

Funding

This work was supported by the National Natural Science Foundation of China (32060645), the Joint Special Project (Key Project) of Local Universities in Yunnan Province (202101BA070000-036), Yunnan Students' innovation and entrepreneurship training program (S202311393052; S202411393039; S202411393055) and the Joint Special Project (Surface Project) of Yunnan Province Local Undergraduate University (202101BA070001-172).

Competing Interests

The authors declare there are no competing interests.

Data availability statement

The data that support the findings of this study are available from the corresponding author upon reasonable request.

Authors' contributions

Yongfu Zhang conceived and designed the experiments. Xiaoxu Bi and Yongfu Zhang the data and wrote the paper. Kai Wang, Xiaoqin Li, Jiao Chen, Jin Yang, Jin Yan and Guijiao Wang performed the experiments. Yongfu Zhang and Xiaoxu Bi contributed equally.

8. References

Ashraf M, Foolad M-R. (2007) Roles of glycine betaine and proline in improving plant abiotic stress resistance. Environmental and Experimental Botany 59: 206-216.

Akcin T A, Akcin A, Yalcn E. (2017) Anatomical changes induced by salinity stress in Salicornia freitagii (Amaranthaceae). Brazilian Journal of Botany 40:1013-1018.

Basu S, Kumar A, Benazir I et al. (2020) Reassessing the role of ion homeostasis for improving salinity tolerance in crop plants. Physiologia Plantarum 171:502-519.

Chen J-H, Chen S-T, He N-Y et al. (2020) Nuclear-encoded synthesis of the D1 subunit of photosystem II increases photosynthetic efficiency and crop yield. Nature Plants 6:570-580.

Dai Y-J, Shen Z-G, Liu Y et al. (2009) Effects of shade treatments on the photosynthetic capacity, chlorophyll fluorescence, and chlorophyll content of Tetrastigma hemsleyanum Diels et Gilg. Environmental & Experimental Botany 65:177-182.

Ding H, Lai J, Wu Q et al. (2015) Jasmonate complements the function of Arabidopsis lipoxygenase3 in salinity stress response. Plant Science 244:1-7.

Dong X-J, Zhang X-S. (2001) Some observations of the adaptations of sandy shrubs to the arid environment in the Mu Us Sandland: leaf water relations and anatomic features. Journal of Arid Environments 48: 41-48.

Estelle M, Salehin M, Li B et al. (2019) Auxin-sensitive Aux/IAA proteins mediate drought tolerance in Arabidopsis by regulating glucosinolate levels. 6:10:4021.

Fu H-Q, Liu X, Song S et al. (2023) Mechanisms of secondary metabolites regulating plant resistance to salinity and alkali stress. Plant Physiology Journal 59: 727-740.

Gamalero E, Bona E, Todeschini V et al. (2020) Saline and Arid Soils: Impact on Bacteria, Plants, and Their Interaction. Biology 9:116.

Gill S-S, Tuteja N. (2010) Reactive oxygen species and antioxidant machinery in abiotic stress tolerance in crop plants. Plant Physiol Biochem 48:909-930.

Guo Y, Jiang Q, Hu Z et al. (2018) Function of the auxin-responsive gene TaSAUR75 under salt and drought stress. The Crop Journal 6:181-190.

Hamada AE, Gaurav Z, Hegab MM et al. (2016) High Salinity Induces Different Oxidative Stress and Antioxidant Responses in Maize Seedlings Organs. Frontiers in Plant Science8:7:276.

He Q. (2019) The Impact of Exogenous Indole-3-acetic Acid on Tea (camellia sinensis (L.) O.kuntze.) Exposed to Cadmium. Agricultural University Of Hunan

Jiang C, Cui Q, Feng K et al. (2016) Melatonin improves antioxidant capacity and ion homeostasis and enhances salt tolerance in maize seedlings. Acta Physiologiae Plantarum 38:1-9.

Joseph GC, Kathleen MB, Jonathan PL. (2014) Reduced Root Cortical Cell File Number Improves Drought Tolerance in Maize. Plant Physiology 166:1943-55.

Jiang W-B, Chen Z, Cao X-L et al. (2019) Effects of exogenous nitric oxide on the growth and membrane lipid peroxidation of Medicago sativa under salt stress. Pratacultural Science 36:2580-2593.

Jue D, Sang X, Liu L et al. (2019) Comprehensive analysis of the longan transcriptome reveals distinct regulatory programs during the floral transition. BMC Genomics 11: 20:126.

Keyikoglu R, Aksu E, Arslan M et al. (2021) Effects of salinity stress on the growth characteristics of four turfgrass species. Fresenius Environmental Bulletin 28:2942-2948.

Kühlbrandt W. (2019) Structure and mechanisms of F-type ATP synthases. Annual Review of Biochemistry 20:88:515-549.
Latoyaharris WT, Newton R. (2003) Molecular Mechanism of Salinity Stress and Biotechnological Strategies for Engineering Salt Tolerance in Plants. Forest Ecosystems 5:52-62.
Li D, Yu X, Jiang X et al. (2010) Effects of 5-azaC on vernalization and flower-ball development in broccoli (Brassica oleracea var. italica). Pakistan Journal of Botany 42: 1889-1893.
Li Z-Q, Hu Y-L, Chang M et al. (2021) 5-azacytidine pre-treatment alters DNA methylation levels and induces genes responsive to salt stress in kenaf (Hibiscus cannabinus L.). Chemosphere 271:129562.
Lin W-H, Lv C-P, Su Y et al. (2012) Exploration on practical skills contest and comprehensive quality cultivation of undergraduates. Experimental Technology and Management 29:4.
Langmead B, Salzberg S-L. (2012) Fast gapped-read alignment with Bowtie 2. Nature Methods 9: 357-359.
Liang X-L, Fang S-M, Ji W et al. (2015) The positive effects of silicon on rice seedlings under saline-alkali mixed stress. Communications in Soil Science and Plant Analysis 46: 2127-2138.
Li X-Y, Liu J, Zhang Y et al. (2009) Physiological responses and adaptive strategies of wheat seedlings to salt and alkali stresses. Soil Science and Plant Nutrition 55:1747-0765.
Li F-L, Bao W-K. (2005) Responses of the Morphological and Anatomical Structure of the Plant Leaf to Environmental Change. Chinese Bulletin of Botany 22:118-127.
Ling L, An Y-M, Wang D et al. (2022) Proteomic analysis reveals responsive mechanisms for saline-alkali stress in alfalfa. Plant Physiology and Biochemistry 1:170:146-159.
Magistretti P-J. (1987) Biochemical approaches to the study of peptide actions. Peptides 17:142-146.
Ogneva ZV, Suprun AR, Dubrovina AS et al. (2019) Effect of 5-azacytidine induced DNA demethylation on abiotic stress tolerance in Arabidopsis Thaliana. Plant Protection Science 55:73-80.
Paheli M, Debasis C. (2021) Adaptation of plants to salt stress: the role of the ion transporters. Journal of Plant Biochemistry and Biotechnology 30:668-683.
Qiu C, Sun J-H, Shen J- Z et al. (2021) Fulvic acid enhances drought resistance in tea plants by regulating the starch and sucrose metabolism and certain secondary metabolism. Journal of Proteomics 15:247:104337.
Ren H-L, Wang X-Y, Zhang F-Y et al. (2023) Salicylic acid and pyraclostrobin can mitigate salinity stress and improve anti-oxidative enzyme activities, photosynthesis, and soybean production under saline-alkali regions. Land 12:1319-1334.
Sadder MT, Alshomali I, Ateyyeh A et al. (2020) Physiological and Molecular Responses for Long Term Salinity Stress in Common Fig (Ficus carica L.). Physiology and Molecular Biology of Plants 27:107-117.
Shin J-H, Mila I, Liu M-C et al. (2019) The RIN-regulated Small Auxin-Up RNA SAUR69 is involved in the unripe-to-ripe phase transition of tomato fruit via enhancement of the sensitivity to ethylene. The New phytologist 222:820-836.
Sharma A, Wang J-F, Xu D-B et al. (2020) Melatonin regulates the functional components of photosynthesis, antioxidant system, gene expression, and metabolic pathways to induce drought resistance in grafted Carya cathayensis plants. Sci Total Environ 15:713:136675.
Wu X-Y, Shu S, Wang Y, Yuan R-N, Guo S- R. (2019) Exogenous putrescine alleviates photoinhibition caused by salt stress through cooperation with cyclic electron flow in cucumber. Photosynthesis Research 141:303-314.

508 Wang X-Y, Zhang Z-X, Gao Y-L, Dong Y-J, Ma X-L, Wang Y-X. (2024) esponse of apple dwarfing rootstocks
509 M9-T337 to exogenous citric acid(CA)under saline and alkaline stresses. Journal of fruit trees 002:041-048.
510 Xi G-Q, Yang X-Z. (1998) Determination of sodium by benzo-15-crown-5-bromocresol green
511 spectrophotometry. analytical chemistry 06:56-59.
512 Xu H-S, Guo S-M, Zhu L et al. (2020) Growth, physiological and transcriptomic analysis of the perennial
513 ryegrass Lolium perenne in response to saline stress. Royal Society Open Science 7:200637.
514 Yang Y-Q, Guo Y. (2018) Elucidating the molecular mechanisms mediating plant salt-stress responses. New
515 Phytol 217:523-539.
516 Yadav V, Wang Z, Wei C et al. (2020) Phenylpropanoid Pathway Engineering: An Emerging Approach
517 towards Plant Defense. Pathogens 23:9:312.
518 Zhang Y, Hou K, Qian H et al. (2022) Characterization of soil salinization and its driving factors in a typical
519 irrigation area of Northwest China. The Science of the total environment 837:155808.
520 Zhu J-K. (2016) Abiotic Stress Signaling and Responses in Plants. Cell 167: 313-324.
521 Zhu M, Lana S, Cuin TA et al. (2016) Nax loci affect SOS1-like Na^+/H^+ exchanger expression and activity in
522 wheat. Journal of Experimental Botany 67:835-844.
523 Zhou H, Liao J, Liu B et al. (2016) Effects of 5-azacytidine and gibberellic acid on flower development of azalea.
524 Pakistan Journal of Agricultural Sciences 53:01-06.
525 Zhong S-L, Fei Z-J, Chen Y-R et al. (2013) Single-base resolution methylomes of tomato fruit development
526 reveal epigenome modifications associated with ripening. Nature Biotechnology 31: 154-159.
527 Zhong L, Xu Y-H, Wang J-B. (2010) The effect of 5-azacytidine on wheat seedlings responses to NaCl stress.
528 Biologia Plantarum 54:753-756.
529 Zoltán Turóczy, Kis P, Trk K et al. (2011) Overproduction of a rice aldo – keto reductase increases oxidative
530 and heat stress tolerance by malondialdehyde and methylglyoxal detoxification[J].Plant Molecular Biology
531 75(4-5): 399-412.
532 Zhao Y, Yang K-J, Li Z-T et al. (2015) Alleviation of salt stress during maize seed germination by presoaking
533 with exogenous sugar. Chinese Journal of Applied Ecology 26: 2735-2742.
534 Zhou W-H, Feng R-Z, Shi S-L et al. (2015) Nitric oxide protection of alfalfa seedling roots against salt-induced
535 inhibition of growth and oxidative damage. Acta Ecologica Sinica 35: 3606-3614.
536 Zhao J, Lang Y, Wu w et al. (2017) Effect of soil extreme drought on photo-physiological and photo-
537 biochemical characteristics of Lonicera japonica Thunb. Acta Botanica Boreali-Occidentalia Sinica 12:
538 2444-2451.
539 Zhu J-K. (2003) Regulation of ion homeostasis under salt stress. Current Opinion in Plant Biology 6: 441-445.
540 Zhu C-C, Shi K, He Q-K et al. (2024) Effectd of mixed saline-alkali stress on physiology and gene expression
541 of alfalfa seedlings. Acta Agrestia Sinica 32:1044-1054.
542 Zhang Y-X, Fan F, Cui L et al. (2012) Effects of saline-alkali stress on the contents of osmotic adjustment and
543 activityof antioxidant enzymes of Carex duriuscula. Grassland and Turf 40:1085-1092.
544 Zhou Q, Guo J-J, He C-T et al. (2016) Comparative Transcriptome Analysis between Low- and High-
545 Cadmium-Accumulating Genotypes of Pakchoi (Brassica chinensis L.) in Response to Cadmium Stress.
546 Environmental Science & Technology 21:50:6485-94.

547 Zou K, Liu X-D, Zhang D et al. (2019) Flavonoid Biosynthesis Is Likely More Susceptible to Elevation and
548 Tree Age Than Other Branch Pathways Involved in Phenylpropanoid Biosynthesis in Ginkgo Leaves.
549 Frontiers in Plant Science 30:10:983.
550 Zhang Y-H, Gao D-P, Wang X- L et al. (2002) The effects of soil salinity on photosystem II of rice seedlings.
551 Journal of Irrigation and Drainage 41:52-60.
552 Zhang Z-S, Yang C, Gao H-Y. (2013) Chilling photoinhibition of photosystem I and its recovery after
553 photoinhibition. Plant Physiology Journal 49:301-308.
554
555

Figure 1

Figure 1

Figure 1. The effect of 5-azacytidine (5-AzaC) treatment on growth condition of *Akebia trifoliata* to saline-alkaline stress. (A): Plant appearance and growth performance of Con, Salt and Salt+5-AzaC. (B): Root growth performance of Con、Salt and Salt+5-AzaC. (C): Agronomic traits of Con, Salt and Salt+5-AzaC. The different letters on the bar chart indicate that by Duncan's new complex range test, the difference reaches a significant level at $P < 0.05$.

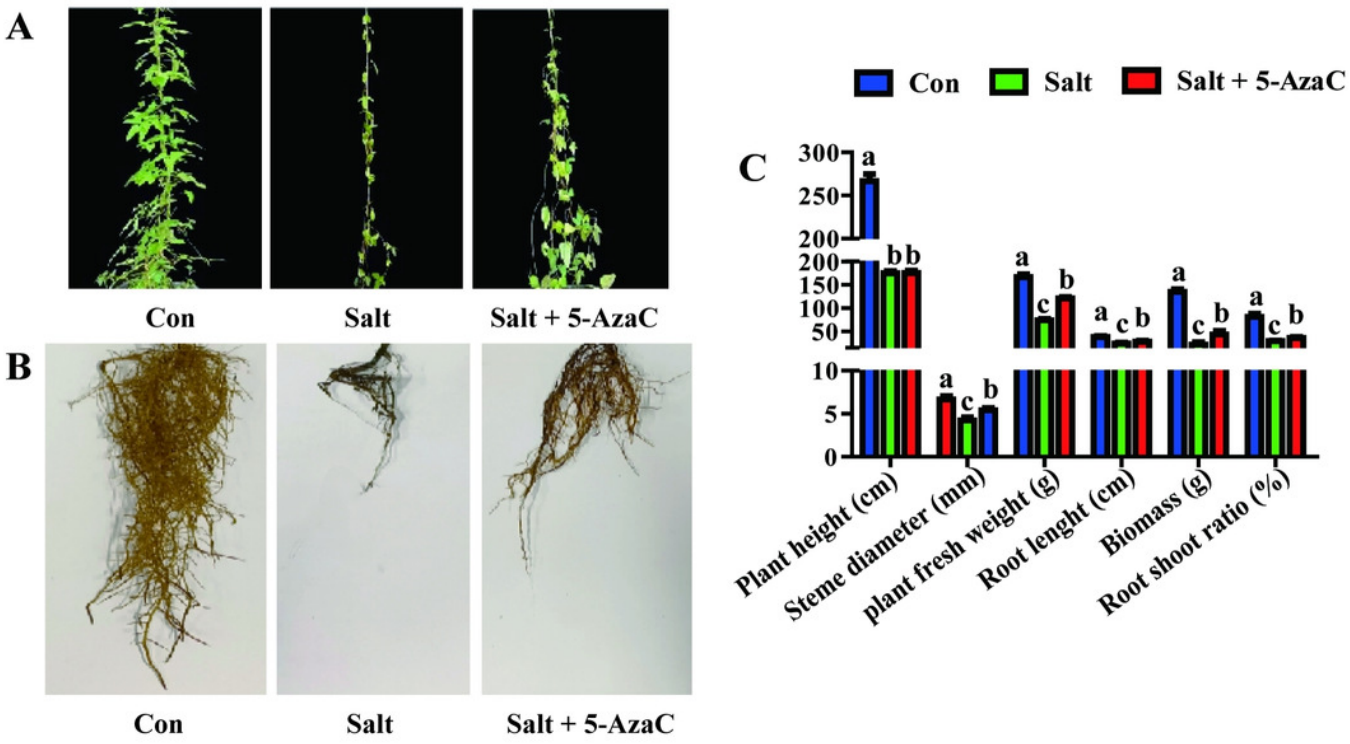

Figure 2

Figure 2

Figure 2. Determination of physiological and biochemical indexes of the leaves of *Akebia trifoliata* treated with 5-AzaC to saline-alkaline stress. (A): The content of Na^+ in leaves of *Akebia trifoliata;* (B-D): The activities of CAT, POD and SOD; E-H: The contents of H_2O_2, MDA,proline and soluble sugar; (I-L): The contents of chlorophyll a, chlorophyll b, total chlorophyll and carotenoid. The results were shown as mean ± standard deviation value (n=4), One-way ANOVA was used to compare the significant differences among the treatments. Different lowercase letters on the bar chart indicated significant differences at the $P < 0.05$ level.

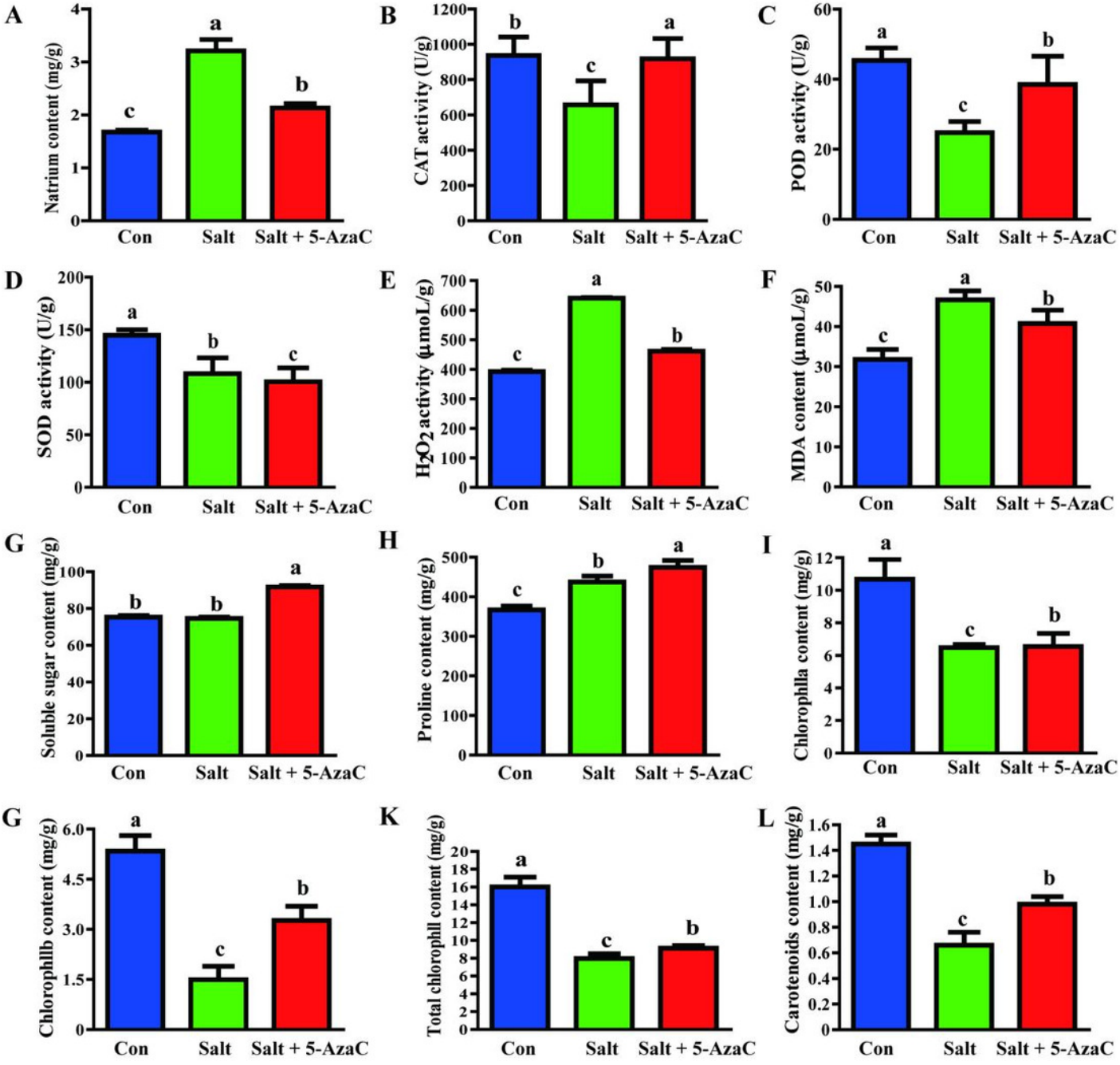
A
Natrium content (mg/g)
c
a
b
Con
Salt
Salt + 5-AzaC
B
CAT activity (U/g)
b
c
a
C
POD activity (U/g)
a
c
b
D
SOD activity (U/g)
a
b
c
E
H2O2 activity (μmoL/g)
c
a
b
F
MDA content (μmoL/g)
c
a
b
G
Soluble sugar content (mg/g)
b
b
a
H
Proline content (mg/g)
c
b
a
I
Chlorophlla content (mg/g)
a
c
b
G
Chlorophllb content (mg/g)
a
c
b
K
Total chlorophll content (mg/g)
a
c
b
L
Carotenoids content (mg/g)
a
c
b

Figure 3

Figure 3

Figure 3. Effects of 5-AzaC on anatomic structure of *Akebia trifoliata* under saline-alkaline stress. The figure of A (Con), B (Salt) and C (Salt+5-AzaC) was shows root structures, a is for cortex, b is for phloem, c is for cambium, d is for xylem, e is for xylem vessel; The figure of D (Con), E (Salt) and F (Salt+5-AzaC) was shows stem structure, a is for cortex, b is for phloem, c is for cambium, d is for xylem, e is for xylem vessel, f is for pith; The figure of G (Con), H (Salt) and I (Salt+5-AzaC) was shows leaf structure, Ue is for upper epidermis, Le is for lower epidermis, Pt is for palisade parenchym, St is spongy tissue, Tp is for thick horn and parenchyma, VB is for vascular bundle, Ph is for phloem, X is for xylem.

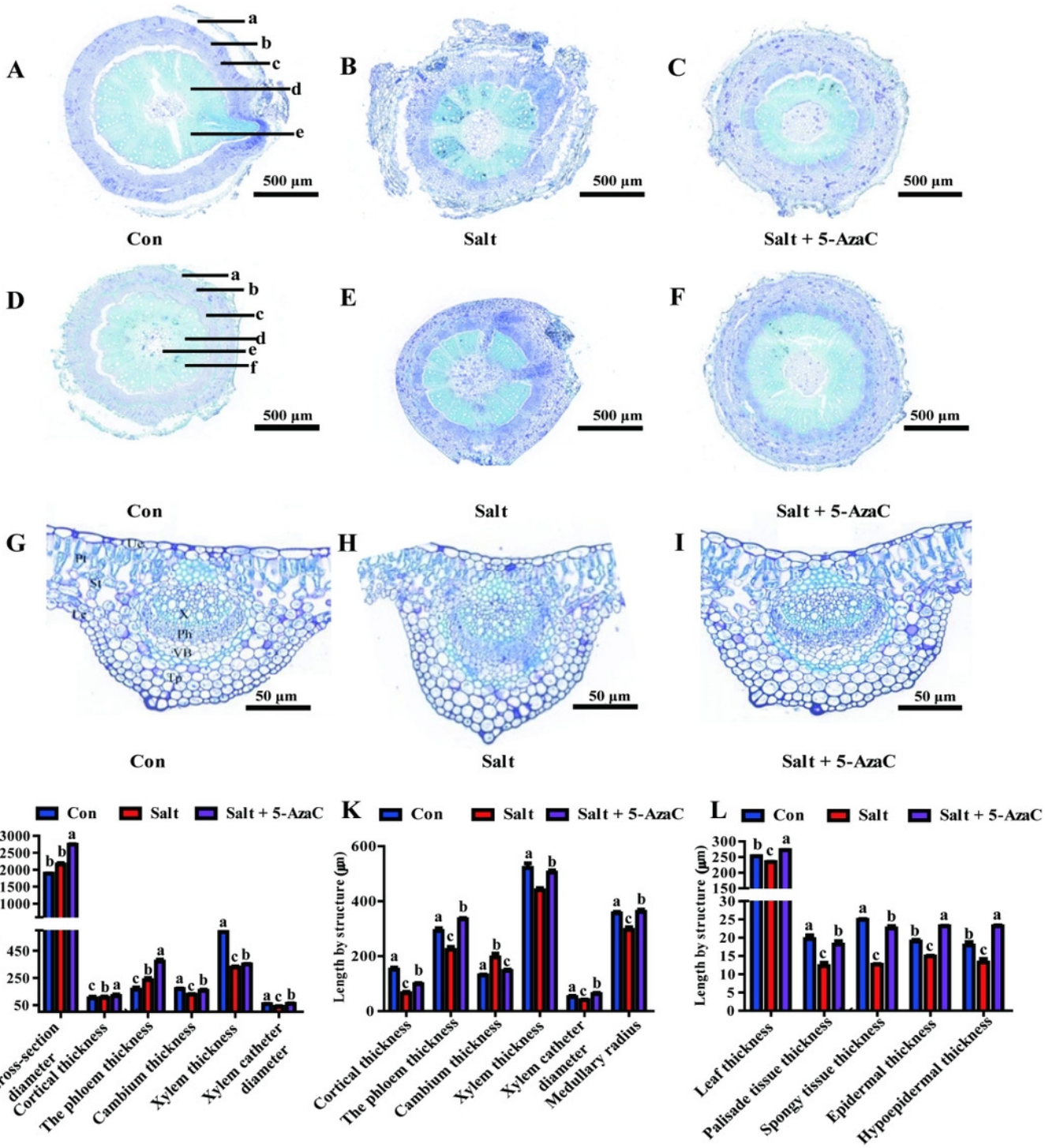
A
a
b
c
d
e
500 μm
Con
B
500 μm
Salt
C
500 μm
Salt + 5-AzaC
D
a
b
c
d
e
f
500 μm
Con
E
500 μm
Salt
F
500 μm
Salt + 5-AzaC
G
Pl
St
Lc
X
Ph
VB
Tp
50 μm
Con
H
50 μm
Salt
I
50 μm
Salt + 5-AzaC
J
Con
Salt
Salt + 5-AzaC
Length by structure (μm)
Root cross-section diameter
Cortical thickness
The phloem thickness
Cambium thickness
Xylem thickness
Xylem catheter diameter
K
Con
Salt
Salt + 5-AzaC
Length by structure (μm)
Cortical thickness
The phloem thickness
Cambium thickness
Xylem thickness
Xylem catheter diameter
Medullary radius
L
Con
Salt
Salt + 5-AzaC
Length by structure (μm)
Leaf thickness
Palisade tissue thickness
Spongy tissue thickness
Epidermal thickness
Hypoepidermal thickness

Figure 4

Figure 4

Figure 4. Effect of 5-azacytidine on *Akebia trifoliata* DEGs under saline-alkali stress. (A) The venn analysis of differential genes among Salt +5-AzaC vs Con, Salt vs Con and Salt +5-AzaC vs Salt; (B) Histogram of differential gene expression analysis between Salt vs Con, Salt +5-AzaC vs Con and Salt +5-AzaC vs Salt; The horizontal coordinate represents different differential comparison groups, the vertical coordinate represents the corresponding number of up-down-regulated genes, the red represents up-regulated, and the blue represents down-regulated.

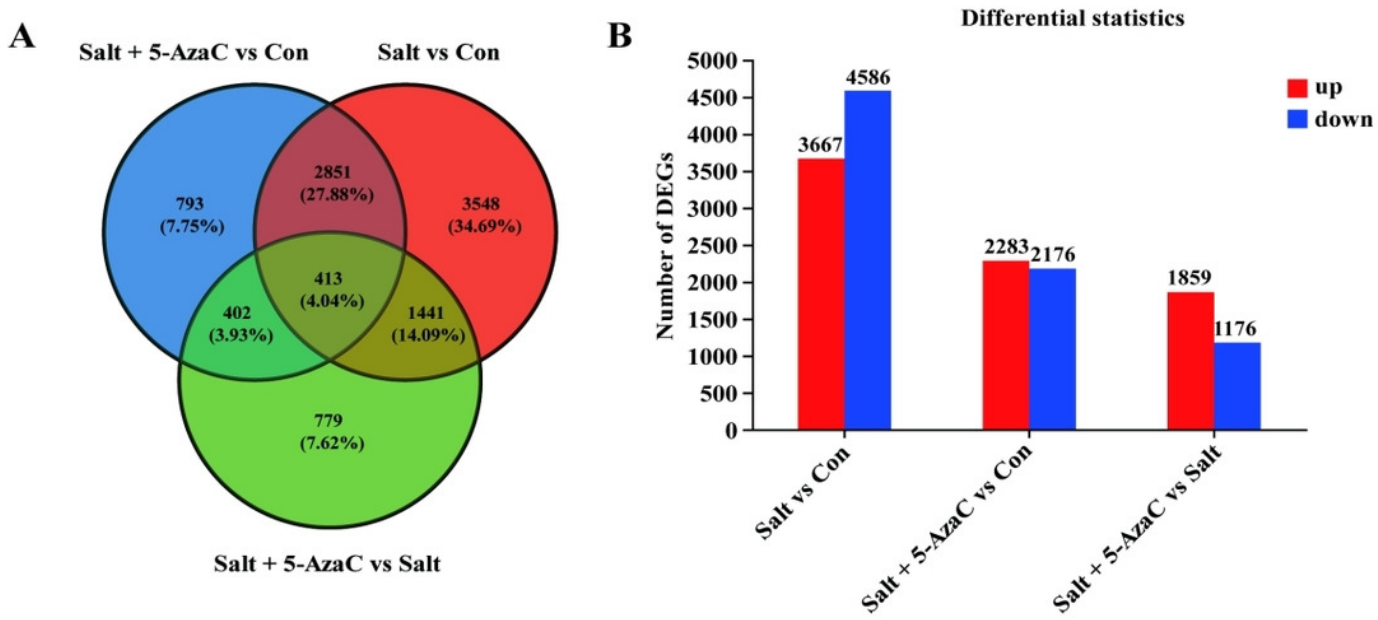

Figure 5

Figure 5

Figure 5. KEGG enrichment analysis of effects of 5-AzaC on DEGs of *Akebia trifoliata* under saline-alkaline stress. (A) KEGG enriched the top 20 signaling pathways of Salt vs Con ($P<0.05$); (B) KEGG enriched the top 20 signaling pathways of Salt +5-AzaC vs Con ($P<0.05$); (C) KEGG enriched the top 20 signaling pathways of Salt +5-AzaC vs Salt ($P<0.05$).

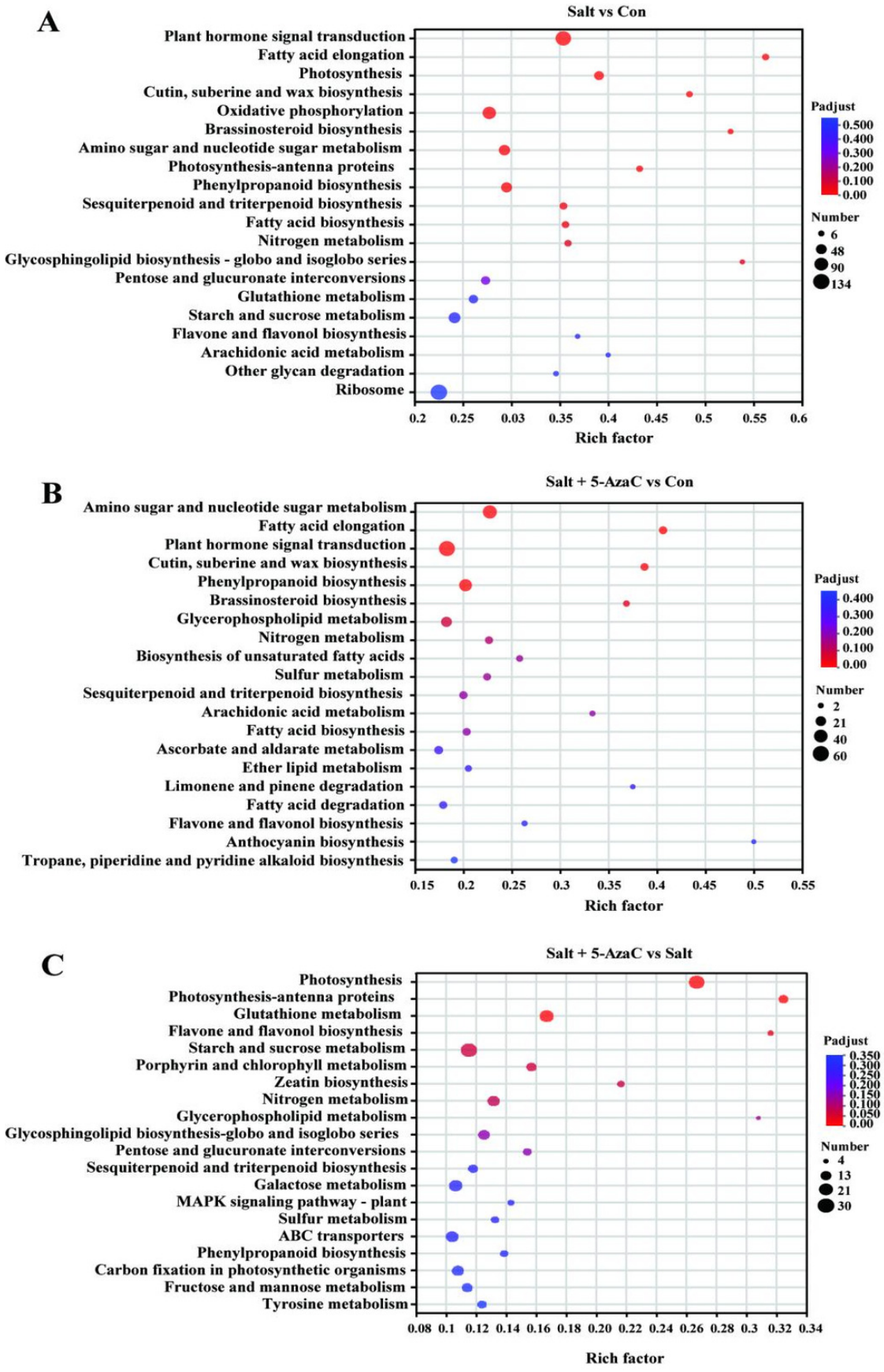
A
Salt vs Con
Plant hormone signal transduction
Fatty acid elongation
Photosynthesis
Cutin, suberine and wax biosynthesis
Oxidative phosphorylation
Brassinosteroid biosynthesis
Amino sugar and nucleotide sugar metabolism
Photosynthesis-antenna proteins
Phenylpropanoid biosynthesis
Sesquiterpenoid and triterpenoid biosynthesis
Fatty acid biosynthesis
Nitrogen metabolism
Glycosphingolipid biosynthesis - globo and isoglobo series
Pentose and glucuronate interconversions
Glutathione metabolism
Starch and sucrose metabolism
Flavone and flavonol biosynthesis
Arachidonic acid metabolism
Other glycan degradation
Ribosome
0.2 0.25 0.03 0.35 0.4 0.45 0.5 0.55 0.6
Rich factor
Padjust
0.500
0.400
0.300
0.200
0.100
0.00
Number
6
48
90
134
B
Salt + 5-AzaC vs Con
Amino sugar and nucleotide sugar metabolism
Fatty acid elongation
Plant hormone signal transduction
Cutin, suberine and wax biosynthesis
Phenylpropanoid biosynthesis
Brassinosteroid biosynthesis
Glycerophospholipid metabolism
Nitrogen metabolism
Biosynthesis of unsaturated fatty acids
Sulfur metabolism
Sesquiterpenoid and triterpenoid biosynthesis
Arachidonic acid metabolism
Fatty acid biosynthesis
Ascorbate and aldarate metabolism
Ether lipid metabolism
Limonene and pinene degradation
Fatty acid degradation
Flavone and flavonol biosynthesis
Anthocyanin biosynthesis
Tropane, piperidine and pyridine alkaloid biosynthesis
0.15 0.2 0.25 0.3 0.35 0.4 0.45 0.5 0.55
Rich factor
Padjust
0.400
0.300
0.200
0.100
0.00
Number
2
21
40
60
C
Salt + 5-AzaC vs Salt
Photosynthesis
Photosynthesis-antenna proteins
Glutathione metabolism
Flavone and flavonol biosynthesis
Starch and sucrose metabolism
Porphyrin and chlorophyll metabolism
Zeatin biosynthesis
Nitrogen metabolism
Glycerophospholipid metabolism
Glycosphingolipid biosynthesis-globo and isoglobo series
Pentose and glucuronate interconversions
Sesquiterpenoid and triterpenoid biosynthesis
Galactose metabolism
MAPK signaling pathway - plant
Sulfur metabolism
ABC transporters
Phenylpropanoid biosynthesis
Carbon fixation in photosynthetic organisms
Fructose and mannose metabolism
Tyrosine metabolism
0.08 0.1 0.12 0.14 0.16 0.18 0.20 0.22 0.24 0.26 0.28 0.3 0.32 0.34
Rich factor
Padjust
0.350
0.300
0.250
0.200
0.150
0.100
0.050
0.00
Number
4
13
21
30

Figure 6

Figure 6

Figure 6. DEGs involved in Plant hormone signal transduction. AUX1: auxin influx carrier; GH3: auxin responsive GH3 gene family; IAA: auxin-responsive protein IAA; ARF: auxin response factor; SAUR: SAUR family protein; TIR1: transport inhibitor response 1.

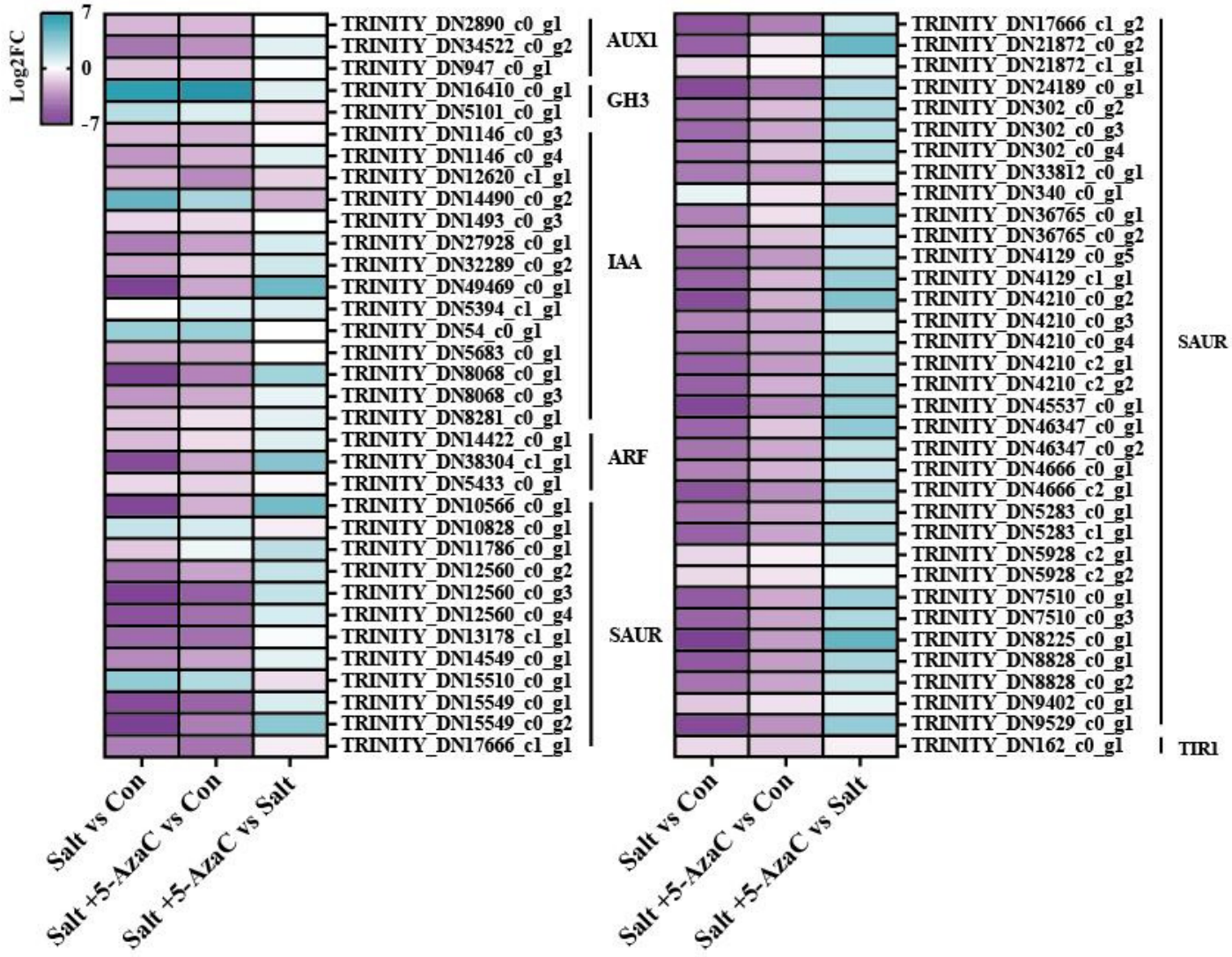

Figure 7

Figure 7

Figure 7. DEGs involved in Phenylpropanoid biosynthesis. E1.11.1.7: peroxidase; E2.1.1.104: caffeoyl-CoA-O-methyltransferase; HCT: shikimate O-hydroxycinnamoyltransferase; E3.2.1.21: beta-glucosidase; REF1: coniferyl-aldehyde dehydrogenase; TOGT1: scopoletin glucosyltransferase; UGT72E: coniferyl-alcohol glucosyltransferase; 4CL: 4-coumarate-CoA ligase; CAD: cinnamyl-alcohol dehydrogenase; COMT: caffeic acid 3-O-methyltransferase; CSE: caffeoylshikimate esterase.

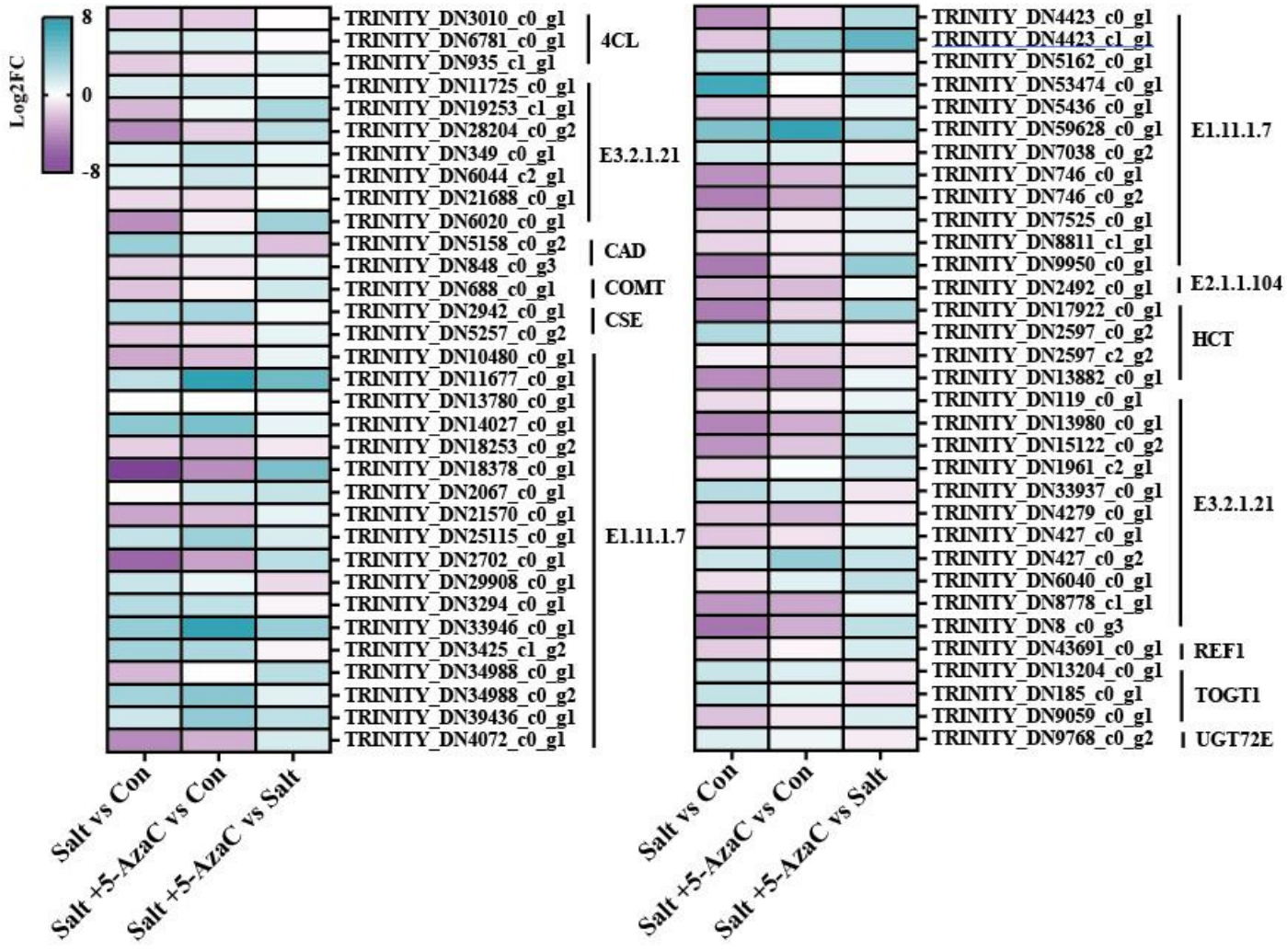

Figure 8

Figure 8

Figure 8. DEGs participating in Photosynthesis. atpF: F-type H^+-transporting ATPase subunit b; atpA: F-type H^+/Na^+-transporting ATPase subunit alpha ; atpH: F-type H^+-transporting ATPase subunit delta; atpG: F-type H^+-transporting ATPase subunit gamma; petA: apocytochrome f; petE: plastocyanin; petF: ferredoxin; petG: cytochrome b6-f complex subunit 5; petH: ferredoxin-NADP+ reductase; psaA: photosystem I P700 chlorophyll a apoprotein A1; psaD: photosystem I subunit II; psaE: photosystem I subunit IV; psaF: photosystem I subunit III; psaG: photosystem I subunit V; psaH: photosystem I subunit VI; psaK: photosystem I subunit X; psaL: photosystem I subunit XI; psaO: photosystem I subunit; psaO; psb27: photosystem II Psb27 protein; psb28: photosystem II 13kDa protein; psbA: photosystem II P680 reaction center D1 protein; psbD: photosystem II P680 reaction center D2 protein; psbE: photosystem II cytochrome b559 subunit alpha; psbO: photosystem II oxygen-evolving enhancer protein 1; psbP: photosystem II oxygen-evolving enhancer protein 2; psbQ: photosystem II oxygen-evolving enhancer protein 3; psbR: photosystem II 10kDa protein; psbS: photosystem II 22kDa protein; psbW: photosystem II PsbW protein; psbY: photosystem II PsbY protein

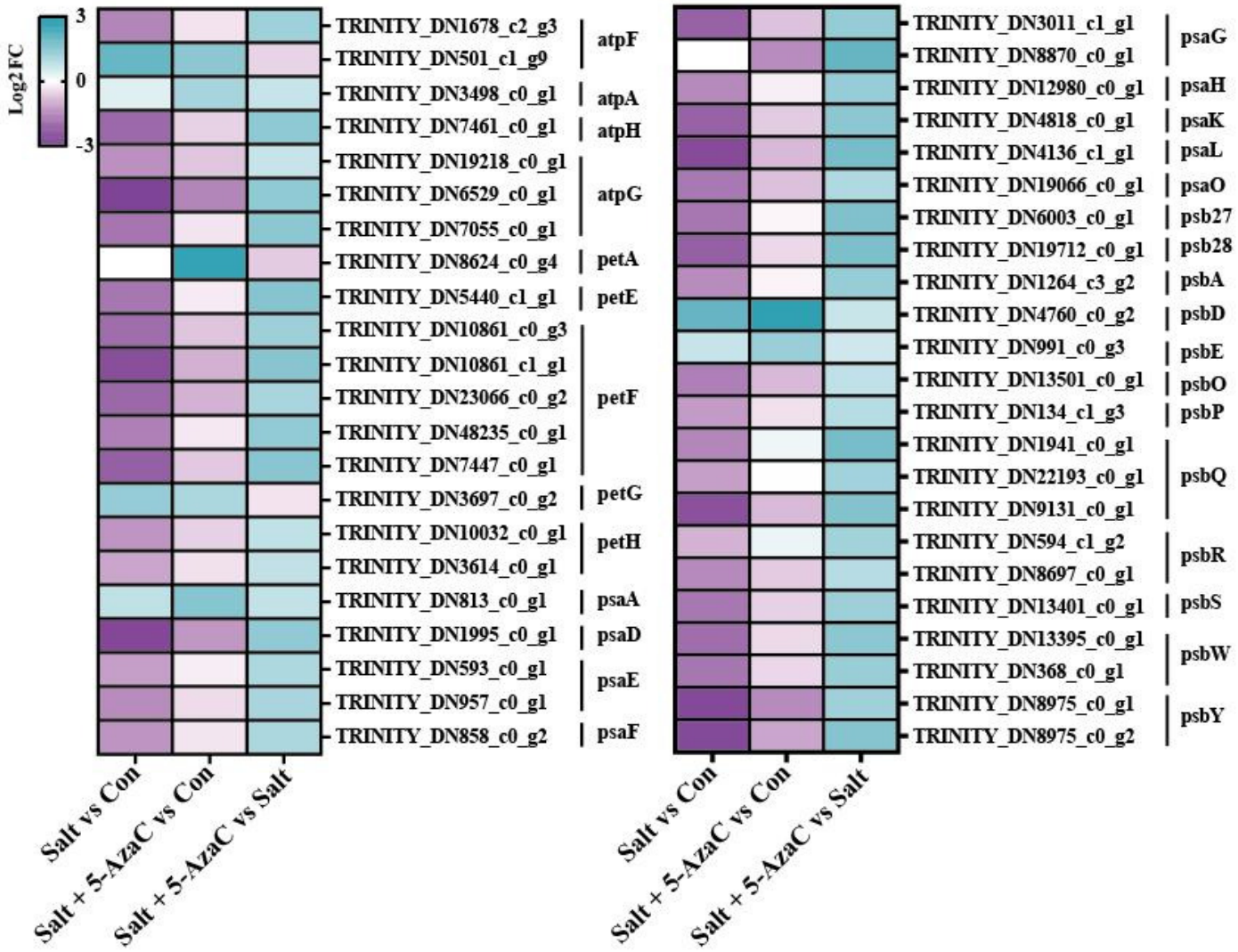
Log2 FC
3
0
-3
TRINITY_DN1678_c2_g3
TRINITY_DN501_c1_g9
TRINITY_DN3498_c0_g1
TRINITY_DN7461_c0_g1
TRINITY_DN19218_c0_g1
TRINITY_DN6529_c0_g1
TRINITY_DN7055_c0_g1
TRINITY_DN8624_c0_g4
TRINITY_DN5440_c1_g1
TRINITY_DN10861_c0_g3
TRINITY_DN10861_c1_g1
TRINITY_DN23066_c0_g2
TRINITY_DN48235_c0_g1
TRINITY_DN7447_c0_g1
TRINITY_DN3697_c0_g2
TRINITY_DN10032_c0_g1
TRINITY_DN3614_c0_g1
TRINITY_DN813_c0_g1
TRINITY_DN1995_c0_g1
TRINITY_DN593_c0_g1
TRINITY_DN957_c0_g1
TRINITY_DN858_c0_g2
atpF
atpA
atpH
atpG
petA
petE
petF
petG
petH
psaA
psaD
psaE
psaF
Salt vs Con
Salt + 5-AzaC vs Con
Salt + 5-AzaC vs Salt
TRINITY_DN3011_c1_g1
TRINITY_DN8870_c0_g1
TRINITY_DN12980_c0_g1
TRINITY_DN4818_c0_g1
TRINITY_DN4136_c1_g1
TRINITY_DN19066_c0_g1
TRINITY_DN6003_c0_g1
TRINITY_DN19712_c0_g1
TRINITY_DN1264_c3_g2
TRINITY_DN4760_c0_g2
TRINITY_DN991_c0_g3
TRINITY_DN13501_c0_g1
TRINITY_DN134_c1_g3
TRINITY_DN1941_c0_g1
TRINITY_DN22193_c0_g1
TRINITY_DN9131_c0_g1
TRINITY_DN594_c1_g2
TRINITY_DN8697_c0_g1
TRINITY_DN13401_c0_g1
TRINITY_DN13395_c0_g1
TRINITY_DN368_c0_g1
TRINITY_DN8975_c0_g1
TRINITY_DN8975_c0_g2
psaG
psaH
psaK
psaL
psaO
psb27
psb28
psbA
psbD
psbE
psbO
psbP
psbQ
psbR
psbS
psbW
psbY
Salt vs Con
Salt + 5-AzaC vs Con
Salt + 5-AzaC vs Salt

Table 1(on next page)

Table 1

Table 1. Transcriptome sequencing quality data of *Akebia trifoliata* treated by 5-AzaC under salt and alkali stress

Table 1. Transcriptome sequencing quality data of *Akebia trifoliata* treated by 5-AzaC under salt and alkali stress

Sample	Clean Bases	Clean Reads	Q20%	Q30%	GC%
Con-1	6497523443	44073089	98.17	94.86	44.10
Con-2	6452067836	43747844	98.17	94.78	44.06
Con-3	6542979049	44398334	98.17	94.87	44.15
Salt-1	6412546931	43599460	97.98	94.32	43.00
Salt-2	6390338026	43376374	98.04	94.5	42.97
Salt-3	6128863841	41613048	98.18	94.87	43.23
Salt+5-AzaC-1	6681928214	45332346	98.06	94.56	43.51
Salt+5-AzaC-2	6610329300	44717082	98.09	94.55	43.95
Salt+5-AzaC-3	6625871183	45157322	97.99	94.42	43.36